International Journal of Thermophysics, Vol. 17, No. 4, 1996

Molar Heat Capacity at Constant Volume of Difluoromethane (R32) and Pentafluoroethane (R125) from the Triple-Point Temperature to 345 K at Pressures to 35 MPa

T. O. Lüddecke[1, 2] and J. W. Magee[1, 3]

Received November 16, 1995

Molar heat capacities at constant volume (C_v) of difluoromethane (R32) and pentafluoroethane (R125) were measured with an adiabatic calorimeter. Temperatures ranged from their triple points to 345 K, and pressures up to 35 MPa. Measurements were conducted on the liquid in equilibrium with its vapor and on compressed liquid samples. The samples were of a high purity, verified by chemical analysis of each fluid. For the samples, calorimetric results were obtained for two-phase ($C_v^{(2)}$), saturated liquid (C_σ or C_x'), and single-phase (C_v) molar heat capacities. The C_σ data were used to estimate vapor pressures for values less than 0.3 MPa by applying a thermodynamic relationship between the saturated liquid heat capacity and the temperature derivatives of the vapor pressure. The triple-point temperature (T_{tr}) and the enthalpy of fusion ($\Delta_{fus}H$) were also measured for each substance. The principal sources of uncertainty are the temperature rise measurement and the change-of-volume work adjustment. The expanded uncertainty (at the two-sigma level) for C_v is estimated to be 0.7%, for $C_v^{(2)}$ it is 0.5%, and for C_σ it is 0.7%.

KEY WORDS: difluoromethane; enthalpy of fusion; heat capacity; pentafluoroethane; triple point; vapor pressure.

1. INTRODUCTION

Accurate values of the heat capacity are valuable for establishing the behavior of the higher-order temperature derivatives of an equation of

[1] Thermophysics Division, Chemical Science and Technology Laboratory, National Institute of Standards and Technology, 325 Broadway, Boulder, Colorado 80303-3328, U.S.A.

[2] Guest researcher from the Institute for Thermodynamics, University of Hannover, Hannover, Germany.

[3] To whom correspondence should be addressed.

0195-928X/96/0700-0823$09.50/0

state. In particular, the heat capacity at constant volume (C_v) is related to the equation of state $p(\rho, T)$ by

$$C_v - C_v^0 = -T\int_0^{\rho}\left(\frac{\partial^2 p}{\partial T^2}\right)_{\rho}\frac{d\rho}{\rho^2} \tag{1}$$

where C_v^0 is the ideal-gas heat capacity. At the present time, only one other report of heat capacity data for difluoromethane and only one report (with 10 data points) for pentafluoroethane were available.

In addition to measurements of heat capacities of the single-phase liquid, heat capacities of the saturated liquid are evaluated from measurements in the two-phase region. We can derive vapor-pressure data from the saturated liquid heat capacities by applying an iterative method with the equation presented by Weber [1]:

$$C_\sigma \approx C' = C'' + \frac{RT}{V''}\left(\frac{dV''}{dT}\right) - T\left(\frac{dV''}{dT}\right)\left(\frac{dp}{dT}\right)_\sigma - V''T\left(\frac{d^2p}{dT^2}\right)_\sigma \tag{2}$$

where C_σ denotes the saturated liquid heat capacity and the superscripts ($'$ and $''$) denote saturated liquid and saturated vapor conditions, respectively. Therefore, heat capacity measurements that cover a wide range of p–ρ–T states as well as two-phase states are useful contributions to the development of equations of state.

In this paper, we report a heat capacity data set for both the single-phase liquid and the saturated liquid region from near the triple-point temperature to the upper limit (345 K) of the apparatus. In addition, we report vapor pressures evaluated from the saturated liquid heat capacity data and measurements of the heat of fusion and triple-point temperature for each substance.

2. MEASUREMENTS

2.1. Apparatus and Procedures

The calorimeter used for these measurements has been described in detail by Goodwin [2] and Magee [3]. A spherical bomb contains a sample of well-established mass. The volume of the bomb, approximately 73 cm^3, is a function of temperature and pressure. A platinum resistance thermometer is attached to the bomb for the temperature measurement. Temperatures are reported on the ITS-90, after conversions from the original calibration on the IPTS-68. Pressures are measured with an oscillating quartz crystal pressure transducer with a range of 0–70 MPa.

Adiabatic conditions are ensured by a high vacuum (3×10^{-3} Pa) in the can surrounding the bomb, by a temperature-controlled radiation shield, and by a temperature-controlled guard ring which thermally anchors the filling capillary and the lead wires to the bomb.

For the heat capacity measurement, a precisely determined electrical energy (Q) is applied and the resulting temperature rise ($\Delta T = T_2 - T_1$) is measured. We obtain the heat capacity from

$$C_v = \left(\frac{\partial U}{\partial T}\right)_v \cong \frac{Q - Q_0 - W_{pv}}{n\,\Delta T} \tag{3}$$

where U is the internal energy, Q_0 is the energy required to heat the empty calorimeter, W_{pv} is the change-of-volume work due to the slight dilation of the bomb, and n is the number of moles enclosed in the bomb. In this work, the bomb was charged with sample up to the (p, T) conditions of the highest-density isochore. The bomb and its contents were cooled to a starting temperature in the single-phase liquid region. Then measurements were performed in that region with increasing temperature until either the upper temperature (345 K) or the pressure limit (35 MPa) was attained. After the bomb was cooled with the sample down to a temperature near the triple point, measurements were begun in the two-phase region and continued into the single-phase region, up to the same limits. At the completion of a run, a small part of the sample was cryopumped into a lightweight cylinder for weighing. The next run was started with a smaller density. A maximum of four runs was measured with one filling of the bomb. When the runs were completed, the remaining sample was discharged and weighed.

A series of such runs from different fillings completes the investigation of the (p, T, C_v) surface. The ranges of the measured data are shown in Fig. 1 for R32 and in Fig. 2 for R125 as (p, T) diagrams. In these figures, the ranges of the C_v data are depicted as the shaded regions. Within these ranges, measurements were performed on eight isochores for 74 state conditions for R32 and on seven isochores for 97 state conditions for R125. Below the shaded regions, the vapor-pressure curve is shown in order to indicate the path of (p, T) states followed by two-phase measurements. For R32, 95 two-phase points were measured from close to its triple point to 342 K, and 85 two-phase points were measured for R125 from close to its triple point to 278 K. A search of the literature uncovered only one source of heat capacity measurements at constant pressure (C_p) for each of R32 and R125. Yomo et al. [4] reported C_p measurements for R32 at temperatures from 275 to 315 K at pressures between 1 and 3 MPa; the (p, T) conditions are depicted as the square symbols in Fig. 1. Wilson et al.

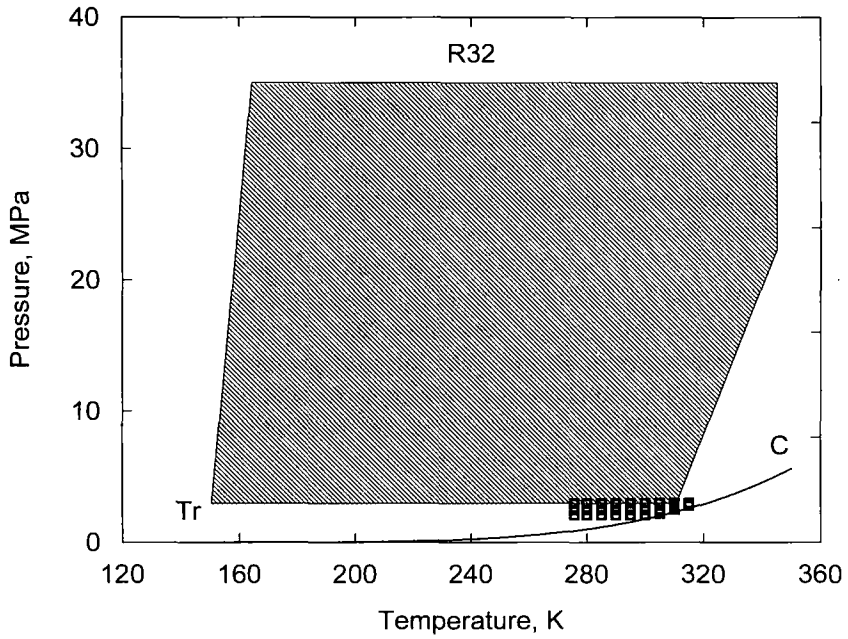

Fig. 1. Range of experimental pressures and temperatures for R32, also showing the values of Yomo et al. [4] (□).

[5] reported C_p measurements for R125 at temperatures from 216 to 333 K on two isobars, at 0.1 and 3.45 MPa; the (p, T) conditions are depicted as the filled circles in Fig. 2.

2.2. Samples

High-purity samples were used for the measurements. The sample of R32 had a purity of 0.9994 mole fraction. The largest impurity was CF_3CH_3 (R143a), with a mole fraction of 0.0004. Other impurities included 100 ppm of CH_3Cl (R40), 10 ppm of $CHCl_2F$ (R21), and 5 ppm of H_2O. The sample of R125 had a purity of 0.99736 mole fraction. The largest impurity was CF_3CClF_2 (R115), with a mole fraction of 0.00263. Other impurities include 2.0 ppm of CO_2, 0.4 ppm of CO, and 1.44 ppm of H_2O. Although the water content of each of these samples was very small, the samples were loaded into thoroughly dried and evacuated cylinders which contained molecular sieves. Subsequent analysis revealed that less than 1 ppm of H_2O remained.

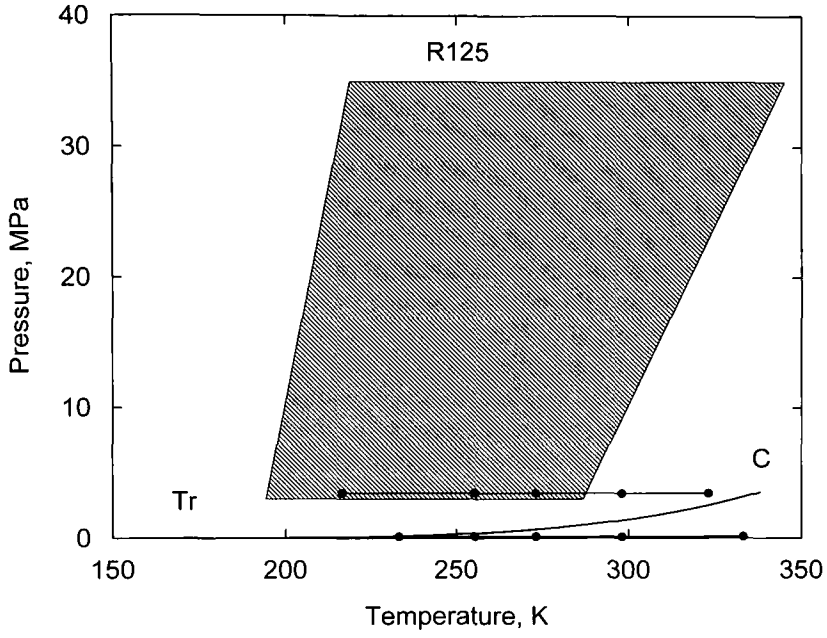

Fig. 2. Range of experimental pressures and temperatures for R125, also showing published values of Wilson et al. [5] (●).

3. RESULTS

3.1. Heat Capacity

As mentioned in Section 2.1, adjustments should be applied to the raw heat-capacity data for the change-of-volume work of the bomb. During a measurement sequence, the volume of the bomb varies with temperature and pressure in accordance with formulas reported previously [2]. It is an important adjustment since the bomb is thin-walled. Referring to Goodwin and Weber [6], we can obtain the work from

$$W_{pv} = \left(T_2 \left(\frac{\partial p}{\partial T} \right)_{V_2} - \frac{1}{2} \Delta p \right) \Delta V \tag{4}$$

where $\Delta p = p_2 - p_1$ is the pressure rise and $\Delta V = V_2 - V_1$ is the change of volume. The pressure derivative is obtained from an equation of state. Precise values for the pressure derivative were required, since this quantity has a significant influence on the adjustment for the change-of-volume work. The first estimates of this derivative were calculated with an extended

corresponding-states model. Then the first iteration of the C_v values were fitted to a preliminary equation of state. The derivatives were recalculated with the preliminary equation of state, leading to better C_v, values. This calculation procedure required four iterations of fitting until the differences in heat capacity from the previous iteration were less than 0.001%.

A minor adjustment is applied to the number of moles enclosed in the bomb. The total mass of the sample weighed is corrected by the amount residing in the noxious volume, which is approximately 0.2% of the bomb volume. This amount is calculated from densities obtained from an equation of state and the noxious volume by using a quadratic temperature profile along the length of the capillary and pressure transducer.

Another minor adjustment is applicable only to the two-phase data. The number of moles residing in the noxious volume changes with the temperature and pressure of the sample in the bomb. In this volume, the substance is in the vapor state. Therefore, the raw heat capacity data must be corrected by the energy spent to evaporate the number of moles driven into the noxious volume during the heating interval.

The heat-capacity data of each run are presented in Tables I and II for two-phase states and in Tables III and IV for single-phase liquid states. For the temperature, the average of the heating interval is given. In the single-phase liquid region, the pressures are calculated from pseudo-isochoric fits of the (p, T) data of each isochore. For these fits, the temperature dependence of the equation of state of Jacobsen and Stewart [8] is used, with the density held constant. In the two-phase region, however, most of the measured vapor pressures are below the range of high accuracy readings of the pressure gauge (3–70 MPa). For this reason, the pressures were calculated from vapor-pressure equations [7] and are not presented as experimental data in the tables. The density, given in Tables III and IV for single-phase liquid states, is calculated from the corrected number of moles and the bomb volume. In Tables I and II, values of the two-phase heat capacity at constant volume ($C_v^{(2)}$) are presented, as well as two types of saturated liquid heat capacities: C'_v (two-phase heat capacity evaluated at ρ_σ) and C_σ [also known as $C'_x = T(dS'/dT)$]. Values of C_σ are obtained by adjusting $C_v^{(2)}$ data with the equation given by Rowlinson [9]:

$$C_\sigma = C_V^{(2)} - \frac{T}{\rho^2}\frac{d\rho_\sigma}{dT}\frac{dp_\sigma}{dT} + T\left(\frac{1}{\rho_\sigma} - \frac{1}{\rho}\right)\frac{d^2 p_\sigma}{dT^2} \tag{5}$$

where ρ_σ and p_σ are the density and the pressure of the saturated liquid and ρ is the bulk density of the sample residing in the bomb. The derivative quantities were calculated with the ancillary equations of Outcalt and McLinden [7].

Table I. Measurements of Heat Capacity C_σ for Saturated Liquid Difluoromethane (R32): T, Temperature (ITS-90); ρ, Density; p, Pressure; $C_v^{(2)}$, Two-Phase Heat Capacity; and C'_v, Two-Phase Heat Capacity Evaluated at the Saturated Liquid Density (Subscript a Denotes a Condition Evaluated at the Average of the Initial and Final Temperatures)

T_a (K)	$\rho_{bulk,a}$ (mol·L^{-1})	$p_{\sigma,a}$ [a] (MPa)	$\rho_{\sigma,a}$ [a] (mol·L^{-1})	$C_v^{(2)}$ (J·mol^{-1}·K^{-1})	C'_v (J·mol^{-1}·K^{-1})	C_σ (J·mol^{-1}·K^{-1})
144.574	12.483	0.000	27.093	82.33	82.32	82.32
149.524	12.480	0.000	26.862	81.96	81.93	81.93
154.425	12.478	0.001	26.632	81.76	81.71	81.71
159.298	12.476	0.001	26.403	81.66	81.59	81.59
164.129	12.473	0.002	26.174	81.51	81.41	81.41
168.924	12.471	0.003	25.946	81.51	81.37	81.37
173.683	12.469	0.004	25.719	81.54	81.34	81.35
178.407	12.466	0.006	25.491	81.61	81.34	81.35
183.094	12.464	0.009	25.264	81.56	81.21	81.22
187.748	12.461	0.013	25.036	81.54	81.10	81.11
192.368	12.459	0.018	24.809	81.71	81.15	81.17
196.957	12.457	0.024	24.580	82.11	81.41	81.44
201.513	12.454	0.033	24.352	82.06	81.21	81.25
206.024	12.452	0.043	24.123	82.59	81.58	81.62
210.511	12.450	0.056	23.893	83.23	82.03	82.09
214.965	12.447	0.072	23.663	83.54	82.14	82.21
219.382	12.445	0.091	23.431	83.75	82.12	82.22
236.578	12.435	0.207	22.500	85.94	83.29	83.53
237.882	12.435	0.219	22.427	86.25	83.51	83.76
240.838	12.433	0.248	22.261	86.41	83.47	83.76
242.140	12.432	0.262	22.187	86.71	83.68	83.98
246.371	12.430	0.312	21.944	87.50	84.16	84.53
250.559	12.427	0.368	21.699	88.40	84.76	85.20
254.716	12.425	0.430	21.452	89.13	85.17	85.71
258.850	12.423	0.501	21.201	90.09	85.81	86.45
262.948	12.420	0.579	20.948	90.95	86.35	87.11
267.014	12.418	0.665	20.690	92.26	87.34	88.23
271.064	12.415	0.760	20.429	92.76	87.52	88.57
275.063	12.413	0.864	20.164	93.83	88.27	89.51
279.043	12.410	0.978	19.893	95.33	89.47	90.92
282.996	12.408	1.102	19.617	96.42	90.25	91.96
286.924	12.405	1.237	19.335	97.41	90.95	92.95
290.822	12.403	1.382	19.047	98.87	92.13	94.48
294.692	12.400	1.539	18.751	100.14	93.15	95.90
298.537	12.397	1.707	18.447	101.41	94.18	97.40
302.353	12.395	1.888	18.134	103.36	95.92	99.70
306.149	12.392	2.082	17.809	104.91	97.28	101.74
309.911	12.389	2.288	17.474	106.04	98.27	103.54
313.648	12.386	2.508	17.124	107.35	99.48	105.74

[a] Calculated from Ref. 7.

Table I. *(Continued)*

T_a (K)	$\rho_{bulk,a}$ (mol·L^{-1})	$p_{\sigma,a}$ [a] (MPa)	$\rho_{\sigma,a}$ [a] (mol·L^{-1})	$C_v^{(2)}$ (J·mol^{-1}·K^{-1})	C'_v (J·mol^{-1}·K^{-1})	C_σ (J·mol^{-1}·K^{-1})
317.344	12.384	2.741	16.759	109.15	101.23	108.70
324.587	12.356	3.246	15.978	112.98	105.15	116.04
328.204	12.353	3.523	15.544	115.64	108.05	121.47
331.770	12.350	3.814	15.078	118.14	110.97	127.79
335.294	12.248	4.120	14.569	120.83	114.30	135.94
338.766	12.345	4.441	14.001	123.91	118.40	147.30
342.173	12.342	4.776	13.349	128.96	125.08	166.04
141.736	17.690	0.000	27.226	82.41	82.40	82.40
145.806	17.687	0.000	27.036	82.07	82.06	82.06
149.846	17.684	0.000	26.847	82.03	82.02	82.02
153.871	17.681	0.001	26.659	81.83	81.81	81.81
157.872	17.679	0.001	26.470	81.75	81.72	81.72
161.853	17.676	0.001	26.282	81.61	81.58	81.58
165.815	17.673	0.002	26.094	81.16	81.11	81.11
169.750	17.671	0.003	25.907	81.18	81.11	81.11
173.672	17.668	0.004	25.719	81.23	81.14	81.15
177.569	17.665	0.006	25.532	81.45	81.34	81.34
181.450	17.662	0.008	25.344	81.33	81.20	81.20
185.307	17.660	0.011	25.156	81.29	81.13	81.14
189.152	17.657	0.014	24.967	81.20	81.00	81.02
192.970	17.654	0.018	24.779	81.39	81.15	81.17
196.774	17.651	0.024	24.590	81.33	81.05	81.07
200.548	17.648	0.031	24.400	81.55	81.23	81.26
204.556	17.645	0.039	24.198	81.80	81.42	81.47
208.785	17.642	0.051	23.982	82.07	81.64	81.69
212.983	17.639	0.064	23.766	82.34	81.83	81.90
217.160	17.636	0.081	23.548	82.66	82.09	82.18
221.312	17.633	0.100	23.329	82.91	82.27	82.38
225.434	17.630	0.123	23.109	83.27	82.56	82.70
229.538	17.626	0.150	22.888	83.58	82.80	82.97
233.609	17.623	0.181	22.665	84.01	83.15	83.36
237.661	17.620	0.217	22.439	84.57	83.64	83.89
241.685	17.617	0.257	22.213	85.05	84.05	84.35
245.685	17.614	0.303	21.984	85.38	84.31	84.67
249.660	17.610	0.355	21.752	85.90	84.78	85.21
253.613	17.607	0.413	21.518	86.31	85.13	85.64
257.543	17.604	0.477	21.281	86.74	85.52	86.12
261.443	17.601	0.549	21.041	87.28	86.02	86.73
265.320	17.597	0.628	20.798	88.21	86.92	87.75
269.186	17.594	0.715	20.551	88.67	87.36	88.34
273.016	17.591	0.810	20.300	89.41	88.11	89.25
276.831	17.587	0.913	20.044	90.05	88.76	90.09
280.621	17.584	1.026	19.784	90.93	89.67	91.22

Table I. *(Continued)*

T_a (K)	$\rho_{bulk,a}$ (mol·L^{-1})	$p_{\sigma,a}$ [a] (MPa)	$\rho_{\sigma,a}$ [a] (mol·L^{-1})	$C_v^{(2)}$ (J·mol^{-1}·K^{-1})	C'_v (J·mol^{-1}·K^{-1})	C_σ (J·mol^{-1}·K^{-1})
284.625	17.580	1.156	19.501	91.68	90.48	92.30
288.835	17.577	1.306	19.195	92.66	91.55	93.71
293.016	17.573	1.469	18.880	93.41	92.43	94.99
297.167	17.569	1.646	18.557	94.70	93.89	96.94
301.295	17.565	1.837	18.222	95.73	95.14	98.76
305.386	17.561	2.042	17.876	96.80	96.49	100.80
141.159	25.440	0.000	27.252	82.53	82.53	82.53
142.852	25.438	0.000	27.174	82.39	82.39	82.39
145.209	25.436	0.000	27.064	82.20	82.20	82.20
150.045	25.432	0.000	26.838	81.95	81.95	81.95
149.243	25.432	0.000	26.875	81.90	81.90	81.90
153.249	25.429	0.000	26.688	81.85	81.85	81.85
157.171	25.425	0.001	26.503	81.81	81.81	81.81
157.246	25.425	0.001	26.500	81.64	81.63	81.63
161.221	25.421	0.001	26.312	81.59	81.59	81.59
165.187	25.417	0.002	26.124	81.70	81.69	81.69
169.134	25.413	0.003	25.936	81.55	81.55	81.55
173.059	25.409	0.004	25.749	81.63	81.63	81.63
176.986	25.405	0.005	25.560	81.26	81.26	81.26

Table II. Measurements of Heat Capacity C_σ for Saturated Liquid Pentafluoroethane (R125): T, Temperature (ITS-90); ρ, Density; p, Pressure; $C_v^{(2)}$, Two-Phase Heat Capacity; and C'_v, Two-Phase Heat Capacity Evaluated at the Saturated Liquid Density (Subscript a Denotes a Condition Evaluated at the Average of the Initial and Final Temperatures)

T_a (K)	$\rho_{bulk,a}$ (mol·L^{-1})	$p_{\sigma,a}$ [a] (MPa)	$\rho_{\sigma,a}$ [a] (mol·L^{-1})	$C_v^{(2)}$ (J·mol^{-1}·K^{-1})	C'_v (J·mol^{-1}·K^{-1})	C_σ (J·mol^{-1}·K^{-1})
180.490	13.568	0.006	13.846	125.53	125.52	125.54
183.989	13.566	0.008	13.752	126.10	126.09	126.11
187.491	13.564	0.010	13.658	125.84	125.84	125.86
181.608	13.134	0.006	13.816	125.02	124.99	125.01
185.182	13.132	0.009	13.720	125.27	125.25	125.26
192.266	13.128	0.015	13.528	126.76	126.73	126.76
195.764	13.126	0.019	13.432	127.61	127.59	127.63
199.258	13.124	0.024	13.335	128.93	128.91	128.96
202.716	13.122	0.029	13.239	129.37	129.35	129.41

[a] Calculated from Ref. 7.

Table II. *(Continued)*

T_a (K)	$\rho_{bulk,a}$ (mol·L^{-1})	$p_{\sigma,a}$ [a] (MPa)	$\rho_{\sigma,a}$ [a] (mol·L^{-1})	$C_v^{(2)}$ (J·mol^{-1}·K^{-1})	C'_v (J·mol^{-1}·K^{-1})	C_σ (J·mol^{-1}·K^{-1})
176.016	12.793	0.004	13.965	124.46	124.43	124.44
179.696	12.791	0.006	13.867	124.80	124.77	124.78
180.113	12.791	0.006	13.856	125.76	125.72	125.73
183.347	12.790	0.007	13.769	125.41	125.37	125.39
183.829	12.789	0.008	13.756	126.12	126.08	126.09
186.970	12.788	0.010	13.672	126.19	126.15	126.17
187.502	12.787	0.010	13.658	126.09	126.05	126.07
190.577	12.786	0.013	13.574	126.76	126.71	126.74
191.168	12.785	0.013	13.558	126.37	126.32	126.34
194.152	12.784	0.017	13.476	127.08	127.03	127.06
194.801	12.783	0.017	13.458	127.96	127.91	127.95
197.705	12.782	0.021	13.378	128.23	128.18	128.22
198.355	12.782	0.022	13.360	128.16	128.11	128.15
201.236	12.780	0.027	13.280	128.47	128.42	128.47
204.740	12.778	0.033	13.182	129.45	129.40	129.47
205.387	12.778	0.035	13.163	129.66	129.61	129.68
208.230	12.776	0.041	13.083	130.10	130.06	130.14
208.873	12.776	0.043	13.064	130.04	130.00	130.09
211.701	12.774	0.050	12.983	130.96	130.93	131.03
212.331	12.774	0.052	12.965	131.07	131.04	131.14
215.143	12.773	0.061	12.884	131.44	131.42	131.54
215.755	12.772	0.063	12.866	132.30	132.28	132.41
175.879	12.409	0.004	13.968	124.64	124.60	124.61
179.621	12.407	0.006	13.869	125.25	125.20	125.21
183.343	12.405	0.007	13.770	125.57	125.52	125.53
187.033	12.403	0.010	13.670	126.19	126.12	126.14
190.698	12.401	0.013	13.571	127.04	126.96	126.99
194.344	12.400	0.017	13.471	127.78	127.70	127.73
197.963	12.398	0.022	13.371	128.04	127.95	127.99
201.555	12.396	0.027	13.271	128.84	128.75	128.80
205.127	12.394	0.034	13.171	129.58	129.47	129.54
208.672	12.392	0.042	13.070	130.58	130.48	130.57
212.198	12.390	0.052	12.969	131.11	131.01	131.12
215.706	12.388	0.063	12.867	131.82	131.72	131.85
219.186	12.387	0.075	12.766	132.50	132.41	132.57
222.656	12.385	0.090	12.663	133.07	132.99	133.18
226.094	12.383	0.107	12.560	133.64	133.59	133.81
229.512	12.381	0.126	12.456	134.53	134.51	134.77
183.158	11.932	0.007	13.774	125.36	125.28	125.29
189.069	11.929	0.012	13.615	126.29	126.18	126.21
194.905	11.926	0.018	13.456	127.73	127.60	127.64
200.698	11.923	0.026	13.295	128.99	128.84	128.89

Table II. *(Continued)*

T_a (K)	$\rho_{bulk,a}$ (mol·L^{-1})	$p_{\sigma,a}$ [a] (MPa)	$\rho_{\sigma,a}$ [a] (mol·L^{-1})	$C_v^{(2)}$ (J·mol^{-1}·K^{-1})	C_v' (J·mol^{-1}·K^{-1})	C_σ (J·mol^{-1}·K^{-1})
206.426	11.920	0.037	13.134	129.75	129.58	129.65
212.081	11.917	0.051	12.972	131.27	131.08	131.19
217.684	11.915	0.070	12.810	132.16	131.96	132.11
223.247	11.912	0.093	12.645	133.23	133.03	133.23
228.762	11.909	0.121	12.479	134.30	134.11	134.37
234.214	11.906	0.156	12.311	135.92	135.76	136.10
239.617	11.903	0.197	12.142	137.01	136.90	137.33
244.988	11.900	0.246	11.969	138.07	138.04	138.59
180.565	11.216	0.006	13.844	125.65	125.54	125.56
185.545	11.214	0.009	13.710	125.82	125.69	125.71
190.468	11.212	0.013	13.577	126.76	126.59	126.62
200.236	11.207	0.025	13.308	129.03	128.79	128.84
205.044	11.205	0.034	13.173	129.84	129.56	129.63
209.837	11.202	0.045	13.037	130.26	129.94	130.03
214.550	11.200	0.059	12.901	131.43	131.07	131.19
219.242	11.198	0.076	12.764	133.02	132.63	132.78
223.885	11.196	0.096	12.626	133.30	132.88	133.08
228.487	11.193	0.120	12.487	134.92	134.47	134.73
237.618	11.189	0.181	12.205	137.51	137.05	137.44
242.133	11.187	0.219	12.061	137.59	137.14	137.62
246.599	11.184	0.262	11.916	139.74	139.31	139.90
251.048	11.182	0.312	11.769	140.29	139.90	140.62
255.439	11.180	0.367	11.620	142.05	141.73	142.60
259.842	11.177	0.430	11.466	143.17	142.93	143.99
264.177	11.175	0.500	11.312	143.41	143.29	144.56
178.294	10.672	0.005	13.904	124.58	124.46	124.47
184.648	10.669	0.008	13.734	125.25	125.08	125.10
190.941	10.666	0.013	13.564	126.84	126.62	126.65
197.149	10.663	0.020	13.394	128.45	128.17	128.21
203.310	10.661	0.030	13.222	129.61	129.26	129.32
209.384	10.658	0.044	13.050	130.48	130.05	130.14
215.402	10.655	0.062	12.876	132.60	132.09	132.22
221.377	10.652	0.084	12.701	133.28	132.70	132.87
227.262	10.650	0.113	12.525	134.34	133.69	133.93
233.105	10.647	0.148	12.346	135.74	135.03	135.34
238.865	10.644	0.191	12.165	137.14	136.38	136.80
244.604	10.641	0.242	11.981	138.91	138.13	138.68
250.292	10.639	0.303	11.794	140.37	139.59	140.28
255.924	10.636	0.374	11.603	141.83	141.08	141.97
261.505	10.633	0.456	11.408	143.77	143.08	144.21
267.022	10.630	0.550	11.208	144.92	144.33	145.76
277.960	10.624	0.778	10.788	148.94	148.72	150.98

Table III. Measurements of Heat Capacity C_v for Liquid Difluoromethane (R32): T, Temperature (ITS-90); ρ, Density; and p, Pressure (Subscript a Denotes a Condition Evaluated at the Average of the Initial and Final Temperatures)

T_a (K)	ρ_a ($mol \cdot L^{-1}$)	p_a (MPa)	C_v ($J \cdot mol^{-1} \cdot K^{-1}$)
152.937	26.838	8.918	53.55
154.936	26.819	13.595	53.36
156.718	26.802	17.741	53.26
158.715	26.784	22.341	53.14
160.481	26.768	26.356	53.05
162.456	26.750	30.787	53.19
166.044	26.210	7.358	52.35
169.870	26.177	15.506	52.00
173.682	26.144	23.505	51.83
177.475	26.112	31.314	51.88
184.343	25.347	6.772	50.72
186.305	25.332	10.465	50.73
188.231	25.317	14.071	50.63
190.186	25.302	17.707	50.66
192.107	25.287	21.252	50.53
194.046	25.272	24.802	50.51
195.960	25.258	28.274	50.52
197.891	25.243	31.746	50.53
203.189	24.475	8.267	49.81
205.352	24.460	11.861	49.72
207.127	24.448	14.769	49.56
209.281	24.433	18.273	49.66
211.043	24.421	21.124	49.55
213.183	24.407	24.570	49.68
214.943	24.395	27.386	49.73
225.139	23.383	7.891	49.03
226.988	23.371	10.494	48.84
229.135	23.359	13.502	48.96
231.000	23.348	16.102	48.93
233.101	23.335	19.014	48.98
234.988	23.324	21.615	48.93
237.056	23.312	24.448	49.00
238.954	23.301	27.030	48.95
240.994	23.289	29.783	49.08
249.175	22.076	6.735	48.49
251.122	22.067	8.992	48.73

Table III. *(Continued)*

T_a (K)	ρ_a (mol · L^{-1})	p_a (MPa)	C_v (J · mol^{-1} · K^{-1})
253.253	22.056	11.449	48.69
255.185	22.046	13.669	48.73
257.314	22.036	16.103	48.75
259.245	22.026	18.303	48.98
261.367	22.016	20.710	48.88
263.276	22.007	22.864	49.08
265.399	21.996	25.249	48.94
267.312	21.987	27.385	49.19
269.416	21.977	29.721	49.21
277.925	20.334	5.777	49.07
279.975	20.326	7.595	48.94
282.096	20.318	9.471	49.25
284.155	20.310	11.287	49.23
286.269	20.302	13.147	49.31
288.339	20.294	14.963	49.28
290.427	20.286	16.790	49.35
292.512	20.278	18.609	49.26
294.581	20.270	20.409	49.50
296.667	20.262	22.218	49.28
298.724	20.254	23.996	49.47
300.808	20.246	25.791	49.53
302.854	20.238	27.547	49.61
304.945	20.230	29.334	50.08
306.972	20.223	31.060	50.11
314.718	17.520	5.239	50.88
316.940	17.514	6.491	50.62
319.143	17.509	7.733	51.00
321.349	17.503	8.980	50.81
323.564	17.498	10.232	50.94
325.771	17.492	11.480	50.82
327.977	17.487	12.728	51.06
330.182	17.481	13.975	50.95
332.389	17.476	15.223	51.06
334.596	17.470	16.471	51.15
336.800	17.464	17.716	51.22
339.005	17.459	18.961	51.10
341.205	17.453	20.201	51.28

Table IV. Measurements of Heat Capacity C_v for Liquid Difluoromethane (R125): T, Temperature (ITS-90); ρ, Density; and p, Pressure (Subscript a Denotes a Condition Evaluated at the Average of the Initial and Final Temperatures)

T_a (K)	ρ_a (mol · L^{-1})	p_a (MPa)	C_v (J · mol^{-1} · K^{-1})
200.226	13.522	10.888	84.64
204.391	13.508	16.418	84.86
208.523	13.495	21.824	86.15
212.629	13.482	27.105	87.52
216.694	13.470	32.244	88.65
214.657	13.086	7.694	86.59
216.279	13.082	9.575	86.14
218.815	13.075	12.515	87.48
220.434	13.070	14.387	87.68
222.959	13.063	17.291	88.51
224.561	13.058	19.122	88.26
227.059	13.051	21.955	89.25
228.655	13.047	23.751	88.45
231.141	13.040	26.531	89.61
232.730	13.035	28.296	89.13
235.169	13.029	30.998	90.42
225.008	12.744	5.125	87.88
227.242	12.738	7.456	87.02
229.172	12.732	9.466	88.30
233.307	12.722	13.748	89.06
235.501	12.716	16.006	88.57
237.414	12.711	17.966	90.34
239.591	12.706	20.185	90.11
241.495	12.701	22.117	90.77
243.673	12.695	24.314	90.36
245.541	12.690	26.188	91.26
247.697	12.685	28.338	91.75
249.568	12.680	30.193	91.85
251.716	12.675	32.309	92.75
239.337	12.351	5.844	89.97
241.314	12.346	7.665	90.40
243.490	12.341	9.665	90.45
245.451	12.337	11.462	91.38
247.619	12.331	13.443	91.09
249.568	12.327	15.217	91.61
251.722	12.322	17.170	91.78
253.641	12.318	18.903	92.39
255.797	12.313	20.840	92.24
257.722	12.308	22.563	93.03
259.848	12.303	24.455	92.63
261.764	12.299	26.153	93.57

Table IV. *(Continued)*

T_a (K)	ρ_a (mol·L^{-1})	p_a (MPa)	C_v (J·mol^{-1}·K^{-1})
263.882	12.294	28.021	93.74
265.777	12.290	29.685	93.76
267.888	12.285	31.530	94.45
269.767	12.281	33.165	94.65
257.297	11.866	7.457	92.71
256.523	11.868	6.845	92.44
260.661	11.859	10.107	93.23
263.788	11.853	12.560	93.73
264.784	11.851	13.339	93.74
268.877	11.843	16.528	94.22
270.185	11.840	17.543	94.49
272.945	11.835	19.677	95.14
276.550	11.827	22.448	95.66
276.996	11.826	22.790	95.63
281.019	11.818	25.857	96.28
282.858	11.815	27.251	96.43
285.016	11.810	28.880	97.05
289.117	11.802	31.957	97.79
288.998	11.803	31.869	97.58
275.718	11.148	4.814	95.55
280.559	11.140	7.829	95.62
281.048	11.139	8.134	95.71
286.333	11.130	11.424	97.00
287.038	11.129	11.862	96.64
291.564	11.122	14.670	98.10
293.497	11.118	15.865	98.48
296.802	11.113	17.903	98.93
299.886	11.108	19.798	99.92
306.258	11.097	23.691	100.05
306.882	11.096	24.070	99.83
311.956	11.088	27.146	101.24
313.866	11.085	28.298	100.69
317.076	11.080	30.228	102.06
320.800	11.074	32.456	101.80
322.155	11.071	33.264	102.61
288.465	10.601	3.792	98.31
293.167	10.594	6.243	98.58
293.834	10.593	6.591	99.22
297.445	10.588	8.474	99.49
299.234	10.586	9.407	99.66
301.712	10.582	10.699	99.08
304.563	10.578	12.185	100.57
305.944	10.576	12.904	99.55
309.916	10.570	14.968	101.66

Table IV. *(Continued)*

T_a (K)	ρ_a (mol · L^{-1})	p_a (MPa)	C_v (J · mol^{-1} · K^{-1})
310.192	10.570	15.111	100.55
314.417	10.564	17.301	101.13
315.233	10.563	17.723	101.85
318.643	10.558	19.485	101.44
320.532	10.555	20.459	102.60
322.871	10.552	21.662	101.62
325.835	10.548	23.184	102.65
327.052	10.546	23.808	102.65
331.091	10.540	25.873	103.19
331.271	10.540	25.966	103.77
335.443	10.534	28.091	104.20
336.355	10.533	28.555	104.01
339.618	10.528	30.211	104.80
341.605	10.525	31.216	104.11

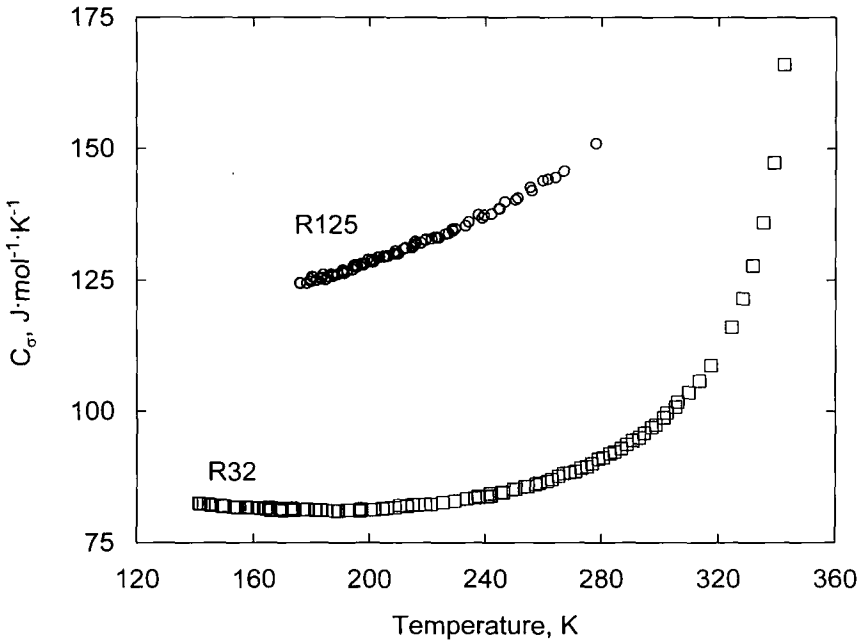

Fig. 3. Experimental saturated liquid heat capacity (C_σ) values for R32 and R125.

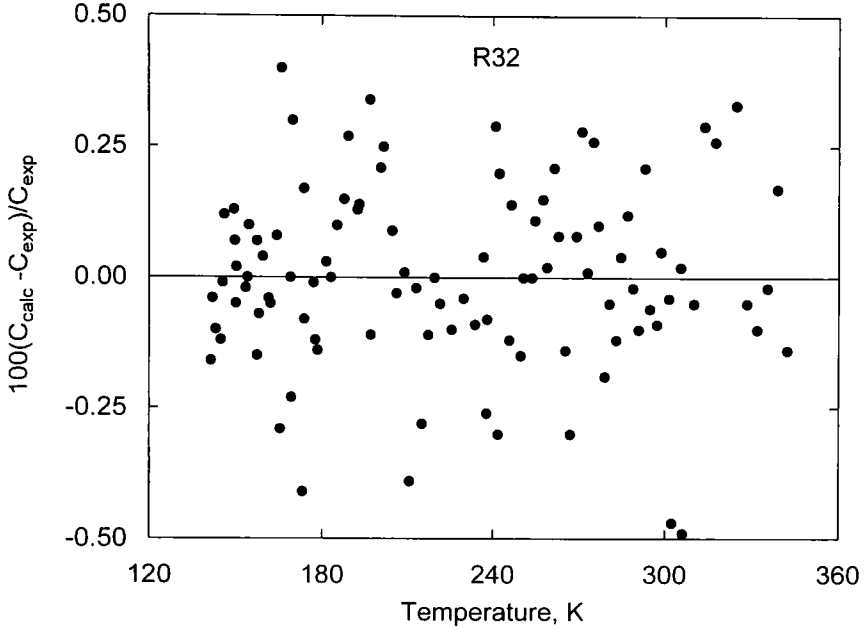

Fig. 4. Comparison of experimental C_σ results for R32 with the values calculated with Eq. (6).

The saturated liquid heat capacity C_σ, as a saturation quantity, depends on a single variable, temperature. If the data are internally consistent, then the values from different isochores must fall on a single curve. Though the C_σ values were evaluated from experiments with different amounts of sample in the calorimeter, the results should demonstrate consistency of all isochores. The saturated liquid heat capacities for all of the filling densities are depicted graphically in Fig. 3. In order to intercompare the data sets from different isochores, an equation which accurately describes the whole data set was derived.

For R32, the four-parameter expression,

$$\ln(C_\sigma/C_0) = a_1 + a_2\tau^{-1/2} + a_3\tau + a_4\tau^{5/4}, \qquad \text{range: } 141 < T < 342 \text{ K} \qquad (6)$$

where $C_0 = 1 \text{ J} \cdot \text{mol}^{-1} \cdot \text{K}^{-1}$, $\tau = 1 - T/T_c$, $T_c = 351.35$ K, $a_1 = 4.4415213$, $a_2 = 0.11555851$, $a_3 = -2.9222563$, and $a_4 = 2.9821034$, was fitted by applying software based on the Wagner method of structural optimization [10]. For R125, the two-parameter expression,

$$\ln(C_\sigma/C_0) = b_1 + b_2\tau^{1/4}, \qquad \text{range: } 176 < T < 278 \text{ K} \qquad (7)$$

where $T_c = 339.33$ K, $b_1 = 5.6932924$, and $b_2 = -1.0456079$, was fitted by applying the same method. The deviations are shown in Figs. 4 and 5. Deviations are distributed randomly over the entire temperature range. The heat capacities from different isochores agree within the uncertainty of the measurements, indicating that there is good internal consistency within each data set.

Another method may be applied to measurements of $C_v^{(2)}$ in order to examine the internal consistency of the data set and, at the same time, extract information on the temperature derivatives of vapor pressures and saturated-phase chemical potentials. For this work, we used the relation

$$\frac{C_v^{(2)}}{T} = -M\frac{d^2\mu}{dT^2} + V_m\frac{d^2p_\sigma}{dT^2} \tag{8}$$

derived by Yang and Yang [11], where M denotes the molecular mass, μ denotes the chemical potential, and V_m denotes the molar volume. This relation implies that $C_v^{(2)}/T$ should be linear versus the molar volume along

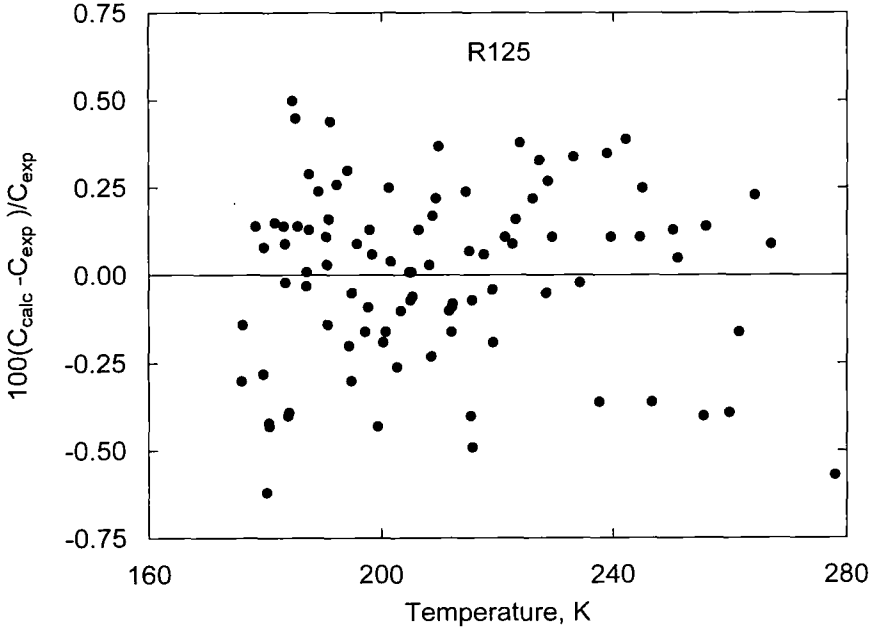

Fig. 5. Comparison of experimental C_σ results for R125 with the values calculated with Eq. (7).

isotherms. Two-phase heat capacity data for R125 are given in Table II to perform this consistency test. We chose to test the five lowest density isochores for R125. Our two-phase heat capacity data for R32 did not cover a broad enough range of densities to warrant this test. For each of the five isochores, the $C_v^{(2)}$ data were fitted to individual equations containing T as the only variable. Then interpolated values were computed at temperatures of 190, 200, 210, 220, 230, and 240 K. These isotherms are shown in Fig. 6. This figure exhibits the linear relationship between the two-phase heat capacity and the molar volume. We note that the y-intercept of each line yields a value for the temperature rate of change of chemical potential μ, and the slope gives a value for the rate of change of the vapor pressure p_σ. Some of the implications of this are rather interesting. First, in this temperature range we may establish, from a knowledge of heat capacity alone, the fact that d^2p_σ/dT^2 is always positive and slowly increasing with increasing temperature. In connection with this fact is that the sign of $d^2\mu/dT^2$ is always negative. To obtain this same information from, for example, vapor pressure measurements would require many closely spaced

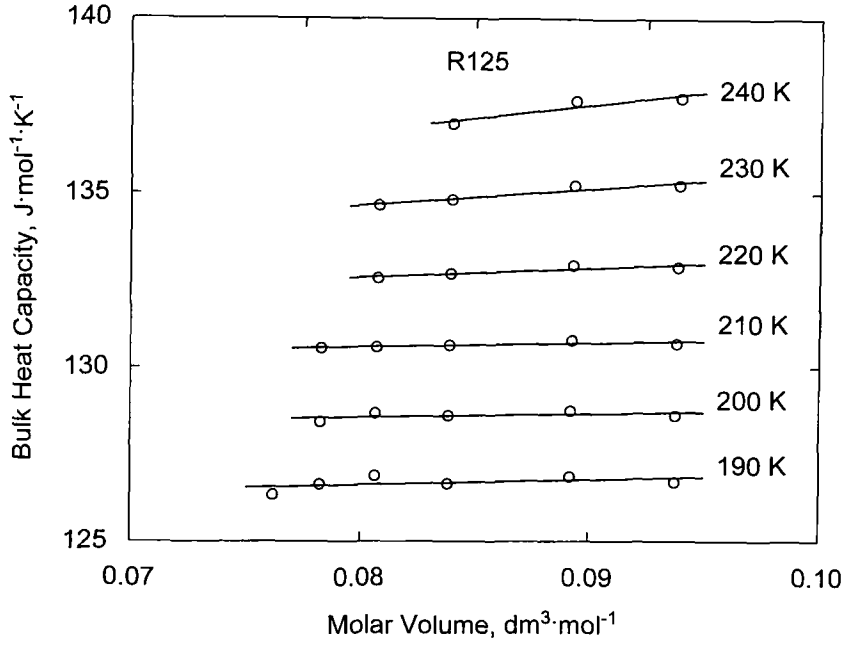

Fig. 6. Interpolated values of two-phase heat capacity ($C_v^{(2)}$) on six isotherms for 125.

measurements of very high accuracy and precision. A knowledge of the second temperature derivative of the vapor pressure curve derived from a calorimetric quantity can assist in the task of accurately fitting vapor pressure data; it may be used to extend the range of temperature or fill in gaps in the existing data.

This technique allows us to make a direct measurement of the internal consistency of the five heat capacity isochores. Most of the values in Fig. 6 are within $0.1\ J \cdot mol^{-1} \cdot K^{-1}$ (0.07%) of the lines fitted to the data. with the largest deviation $0.3\ J \cdot mol^{-1} \cdot K^{-1}$ (0.2%). The slope of the lines, obtained from the fit to each isotherm, was compared to the second derivative of the vapor pressure equation of Outcalt and McLinden [7]. Results are given in Table V. The vapor pressure second derivatives have relatively small values ($<0.3\ kPa \cdot K^{-2}$) at the low reduced temperatures ($0.56 < T/T_c < 0.71$) studied in this work. The derivatives calculated by each of the two methods have the same sign and agree within approximately $\pm 0.06\ kPa \cdot K^{-2}$.

Values of the single-phase liquid heat capacity are shown in Fig. 7. The data are presented on isochores in a C_v–T diagram. Most isochores overlap in their temperature ranges. Figure 7 shows that for R125, the slope of each C_v–T isochore is nearly independent of the density of the isochore. Thus, almost all of the R125 data fall on a single line. The R32 data, however, show a distinctly different dependence on density. Figure 7 depicts a shallow minimum in the range of liquid densities covered by this study. A minimum is also seen in the values of the saturated liquid heat capacity (Fig. 3) at about 190 K. Figure 7 also shows that the variation of

Table V. Comparison of the Vapor Pressure Second Derivatives d^2p_σ/dT^2 for Pentafluoroethane (R125) from Heat Capacity Measurements with Values from Published Vapor Pressures

	d^2p_σ/dT^2 ($kPa \cdot K^{-2}$)		
T (K)	This work	σ^a	Calculated[b]
190.0	0.081	0.001	0.055
200.0	0.050	0.0006	0.085
210.0	0.058	0.0003	0.122
220.0	0.123	0.0004	0.167
230.0	0.211	0.0005	0.218
240.0	0.317	0.0009	0.275

[a] Standard uncertainty of the linear fit.
[b] Outcalt and McLinden [7].

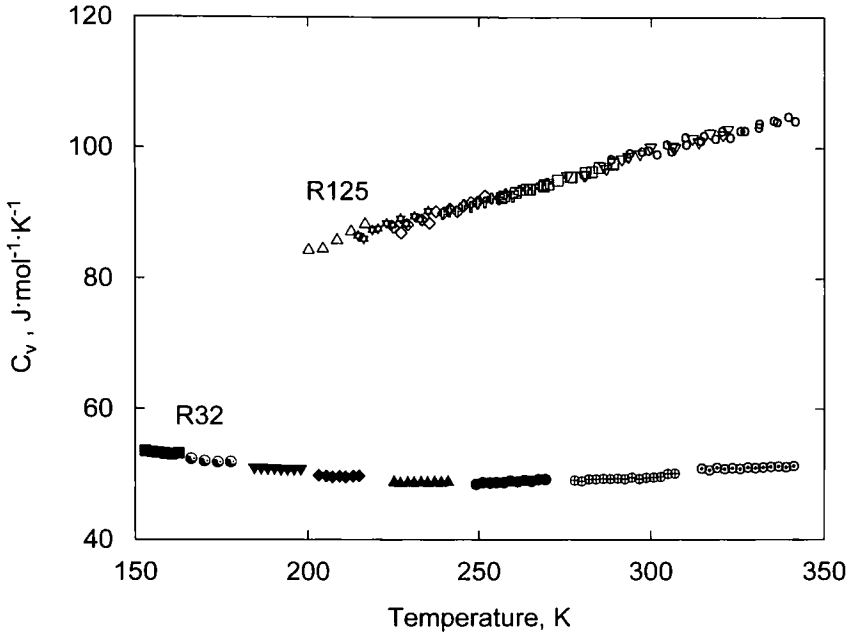

Fig. 7. Experimental liquid-phase heat capacity (C_v) data for R32 and R125.

C_v with temperature and with density is exceptionally weak. Both the observed weak temperature dependence and the existence of a minimum are anomalous for this class of substances. The shape of the (C_v, ρ, T) surface for R32 bears a strong resemblance to that of CO_2 (a quadrupolar molecule) measured with the same apparatus [12]. The exact reason for this similarity is not yet clear. While CO_2 has no dipole moment, R32 is strongly dipolar, exhibiting a gas phase dipole moment p of $(6.598 \pm 0.023) \times 10^{-30}$ C·m (1.978 ± 0.007 D) [13]. In fact, R32 is considerably more dipolar than R125, $(5.214 \pm 0.017) \times 10^{-30}$ C·m (1.563 ± 0.005 D) [14].

Figures 8 and 9 show comparisons of C_v in Tables III and IV with the equations of state of Outcalt and McLinden [7]. These comparisons show the exceptional quality of their equation of state fits for both R32 and R125 data; most of the calculated values of C_v are within 1% of the measurements. At the time this document was prepared, the only other published heat capacity data for R32 and R125 are the two sets of isobaric heat capacity (C_p) data mentioned earlier. Though of high accuracy, these other published values were not used in Outcalt and McLinden's fits; thus, their

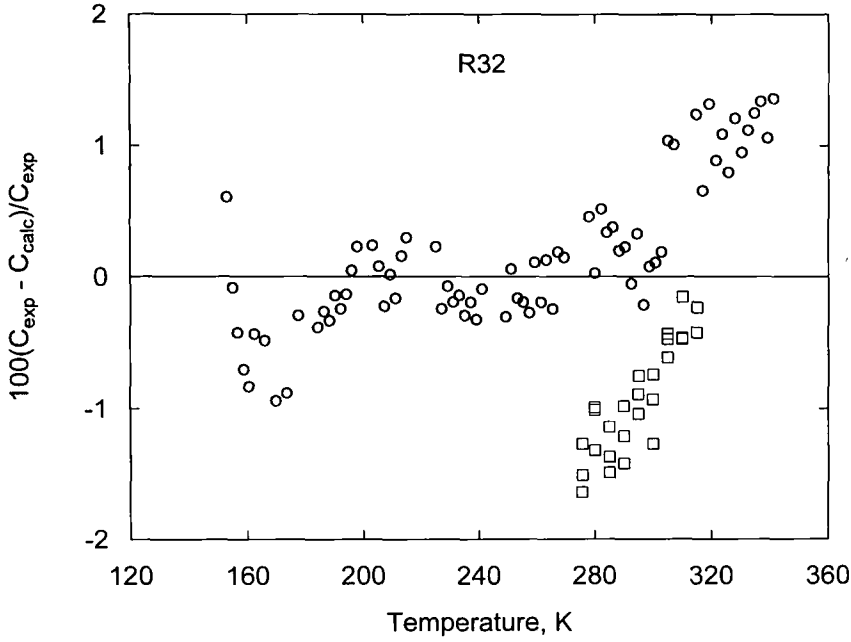

Fig. 8. Comparison of experimental C_v data for R32 from this work (○) and other C_p data [4] (□) with the values calculated using an equation of state [7].

equations of state will facilitate an indirect comparison with published data. The values of Yomo et al. [4] for R32 are expected to have an uncertainty of 0.4%. Wilson et al. [5] claimed an uncertainty of 2% for their C_p values. To make comparisons with this work, we used the equations of state to convert these C_p values to C_v. The deviations of these converted values are also shown in Figs. 8 and 9. This comparison demonstrates that the values of Yomo et al. are close to this work. In their temperature range ($275 < T < 315$ K), the root-mean-square deviation of the heat capacities of this work is 0.54%, while theirs is 1.02%. Figure 8 suggests that the largest difference between this work and that of Yomo et al. is approximately 1.5%. The values of Wilson et al. are within 5% of this work, with 8 of 10 values within ± 2%. Taken as a whole; this work is in good agreement with published data for R32 and R125. We should caution, however, that no published heat capacity data were found for R32 in the temperature range $136 < T < 275$ K or for R125 in the range $172 < T < 216$ K. To validate the measurements from this study which fall in the gaps, new calorimetric data obtained with other accurate experimental methods are desirable.

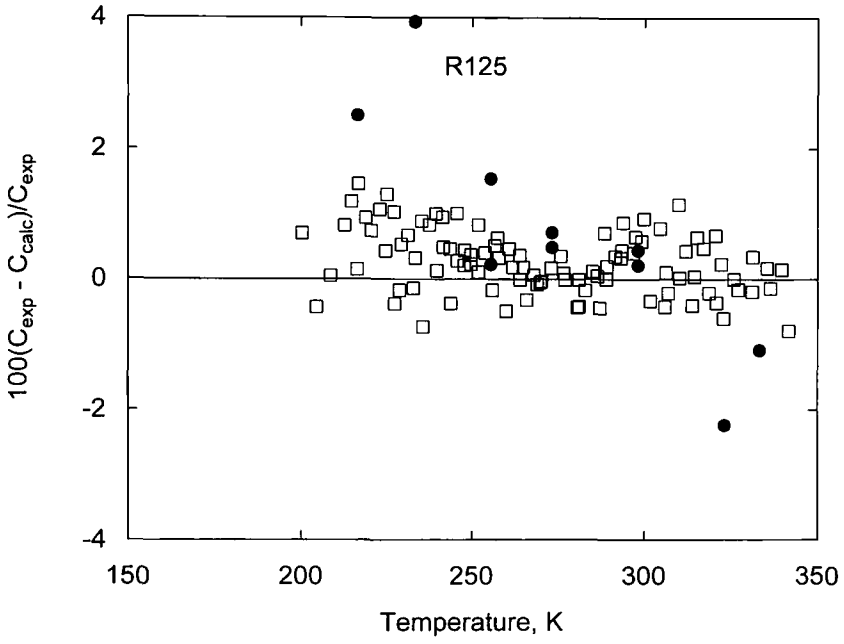

Fig. 9. Comparison of experimental C_v data for R125 from this work (□) and other C_p data [5] (●) with the values calculated using an equation of state [7].

3.2. Derived Vapor Pressures

Vapor pressures measured between the triple point and the normal boiling point with traditional techniques are often inaccurate. In some cases, volatile impurities concentrate in the vapor phase [1]. This will influence the vapor pressure measurement, making it appear larger than the true value for the pure substance. In other instances, the pressure gauges are not accurate enough under these low-pressure conditions. This situation can be remedied to some extent, however, by extracting vapor pressure values from saturated liquid heat capacity measurements. These C_σ values have a high internal consistency and can be accurate below the normal boiling point because the adjustments to the $C_v^{(2)}$ measurements are less than 2% of the resulting C_σ value. We extracted vapor pressures from the data in Tables I and II by applying a method discussed by Baehr [15] and applied recently by Weber [1] using Eq. (2). These results are given in Table VI for R32 and in Table VII for R125. Because the method employed by Weber [1] requires a knowledge of the density of the saturated vapor

Table VI. Vapor Pressure Values for Difluoromethane (R32) Derived from C_σ Measurements

T (K)	p_σ (kPa)
140.000	0.081
145.000	0.165
150.000	0.319
155.000	0.584
160.000	1.026
165.000	1.731
170.000	2.818
175.000	4.442
180.000	6.798

and its first temperature derivative, the expanded uncertainty of the derived vapor pressures is estimated to be ± 0.05 kPa.

3.3. Triple Points

The triple-point temperature of R32 was measured on three samples. No other published data were available. For these experiments, the sample was slowly cooled to a temperature about 2 K below where freezing was noted. Then the solidified sample was heated at a constant power of between 0.09 and 0.25 W. In order to obtain a slowly increasing temperature, heater power was set to a value which is less than one-tenth of the power for heat

Table VII. Vapor Pressure Values for Pentafluoroethane (R125) Derived from C_σ Measurements

T (K)	p_σ (kPa)
170.000	2.333
180.000	5.680
190.000	12.397
200.000	24.690
210.000	45.518
220.000	78.602
230.000	128.395
240.000	200.017
250.000	299.186

capacity experiments. Data evaluation was done graphically. The triple point was located by noting a sharp break in the rate of temperature rise, delineating when melting began. The results and their expanded uncertainties for T_{tr} of the three samples were 136.35 ± 0.02, 136.32 ± 0.02, and 136.35 ± 0.02 K. Thus the average of 136.34 ± 0.03 K was adopted for T_{tr} of R32. The enthalpy of fusion $\Delta_{fus}H$ was measured by integrating the applied heater power over the time of heating and applying a correction for estimated heat losses. Results and their expanded uncertainties for $\Delta_{fus}H$ obtained from the three runs were 4394 ± 130, 4374 ± 130, and 4300 ± 130 J · mol^{-1}; the average of 4356 ± 130 J · mol^{-1} is the best estimate for $\Delta_{fus}H$ at the triple point. Since we did not see a dependence of T_{tr} or $\Delta_{fus}H$ on heater power, it was decided that future melting experiments would be carried out at a fixed power of 0.09 W.

The triple-point temperature of R125 was measured on two samples. At the time of this work, no other published values were available. A similar method was used. The power to the bomb heater was 0.09 W. The results and their expanded uncertainties for T_{tr} of the two samples were 172.53 ± 0.02 and 172.51 ± 0.02 K. As a result, the average of 172.52 ± 0.03 K was adopted for T_{tr} of R125. The results and their expanded uncertainties for $\Delta_{fus}H$ obtained from the two runs were 2254 ± 45 and 2244 ± 45 J · mol^{-1}; the average of 2249 ± 45 J · mol^{-1} is the best estimate for $\Delta_{fus}H$ at the triple point.

3.4. Assessment of Uncertainties

Uncertainty in C_v arises from several sources. Primarily, the accuracy of this method is limited by the uncertainty of the temperature rise measurement and the change-of-volume work adjustment. In the following discussion, we have adopted a definition for the expanded uncertainty which is $\pm 2\sigma$, or two times the standard uncertainty. In other words, the expanded uncertainty has a coverage factor of 2. When we discuss uncertainties in this context, we mean this definition of expanded uncertainty at the two-sigma level.

Different sources, including calibration of the platinum resistance thermometer, radiation to or from the thermometer head, and drift of the ice point resistance, contribute to an expanded uncertainty of $\sigma_t = \pm 0.01$ K at 100 K to ± 0.3 K at 345 K for the absolute temperature measurement. Uncertainty of the temperature rise, however, also depends on the reproducibility of temperature measurements. The temperatures assigned to the beginning (T_1) and to the end (T_2) of a heating interval are determined by extrapolation of a linear temperature drift (approximately -1.0×10^{-3} to 0.5×10^{-3} K · min^{-1}) to the midpoint time of the interval. This procedure

leads to an uncertainty of ± 0.001 to ± 0.004 K for the extrapolated temperatures T_1 and T_2, depending on the standard deviation of the linear function correlated. In all cases, values from ± 0.002 to ± 0.006 K were obtained for the uncertainty of the temperature rise, $\Delta T = T_2 - T_1$. For a typical experimental value of $\Delta T = 4$ K, this corresponds to an uncertainty of ± 0.05 to $\pm 0.15\%$.

The uncertainty of the change-of-volume work influences primarily the single-phase values since two-phase experiments are performed over a small pressure interval. For R32, the ratio of change-of-volume work to total applied heat may be as large as 0.060 for the highest density isochore down to 0.012 for the lowest density. For R125 this range is smaller, 0.007 to 0.028. Estimated uncertainties of ± 2.3 to $\pm 3.0\%$ in the change-of-volume work are due to both the deviation of the calculated pressure derivatives and the uncertainty of the volume change. This leads to an uncertainty of $\pm 0.2\%$ in C_v for the lowest density isochore up to $\pm 0.3\%$ for the highest density.

The energy applied to the calorimeter is the integral of the product of voltage and current from the initial to the final heating time. Voltage and current are measured 20 times during a heating interval. The measurements of the electrical quantities are accurate within approximately $\pm 0.01\%$. However, we must account for the effect of radiation heat losses or gains which occur when a time-dependent lag of the controller leads to a small temperature difference of about 20 mK between bomb and radiation shield at the beginning and end of a heating period. Since heat transfer by radiation is proportional to $T_1^4 - T_2^4 \cong 4T^3 \Delta T$, we would expect radiation losses to increase substantially with the bomb temperature. Therefore, the uncertainty in the applied heat is estimated to be $\pm 0.02\%$ for lower temperatures and up to $\pm 0.10\%$ for the highest temperatures. This leads to an uncertainty between ± 0.04 and $\pm 0.20\%$ in C_v.

Other sources of uncertainty are smaller. The energy applied to the empty calorimeter has been measured in repeated experiments and fitted to a function of temperature [3]; its uncertainty is less than $\pm 0.02\%$. Its influence on the uncertainty of the heat capacity is reduced, because the ratio of the heat applied to the empty calorimeter to the total heat varies only from 0.45 to 0.51 for the single-phase runs and from 0.36 to 0.42 for the two-phase runs. The mass of each sample was determined within $\pm 0.01\%$ by differential weighings before and after trapping the sample. The density calculated from this mass and the bomb volume has an uncertainty of approximately $\pm 0.2\%$. For pressures, the uncertainty of the gauge of ± 7 kPa is added to the cross term for the pressure derivative in the change-of-volume work adjustment. However, the uncertainty of neither p nor ρ contributes appreciably to the combined uncertainty for

molar heat capacity. The expanded uncertainty of C_v is estimated to be 0.7%, by combining the various sources of experimental uncertainty using a root-sum-of-squares formula; for $C_v^{(2)}$ it is 0.5%, and for C_σ it is 0.7%.

4. CONCLUSIONS

For difluoromethane (R32), we have reported 73 C_v, 101 C_σ, 9 p_σ, 3 T_{tr}, and 3 $\Delta_{vap}H$ values. For pentafluoroethane (R125), we have reported 99 C_v, 93 C_σ, 9 p_σ, 2 T_{tr}, and 2 $\Delta_{vap}H$ values. No other published triple points or enthalpies of fusion were found. Two-phase heat capacities for R125 were internally consistent within 0.3 $J \cdot mol^{-1} \cdot K^{-1}$. Agreement with published liquid-phase heat capacity values at constant pressure was within 1.5% for R32 and 5% for R125.

ACKNOWLEDGEMENTS

We are grateful to Mark McLinden and Stephanie Outcalt for generous technical assistance and helpful discussions during this study. We acknowledge the financial support of the Air Conditioning and Refrigeration Technology Institute. We thank the Ernest-Solvay Foundation for financial support of Torsten Lüddecke during his guest researcher appointment at NIST. We have profited from many discussions with W. M. Haynes, Arno Laesecke, Ben Younglove, Marcia Huber, and Lloyd Weber.

REFERENCES

1. L. A. Weber, *Int J. Refrig.* **17**:117 (1992).
2. R. D. Goodwin, *J. Res. Natl. Bur. Stand. (U.S.)* **65C**:231 (1961).
3. J. W. Magee, *J. Res. Natl. Inst. Stand. Technol.* **96**:725 (1991).
4. M. Yomo, H. Sato, and K. Watanabe, *High Temp.-High Press.* **26**:267 (1994).
5. L. C. Wilson, W. V. Wilding, G. M. Wilson, R. L. Rowley, V. M. Felix, and T. Chisolm-Carter, *Fluid Phase Equil.* **80**:167 (1992).
6. R. D. Goodwin and L. A. Weber, *J. Res. Natl. Bur. Stand. (U.S.)* **73A**:1 (1969).
7. S. L. Outcalt and M. O. McLinden, *Int. J. Thermophys.* **16**:79 (1995).
8. R. T. Jacobsen and R. B. Stewart, *J. Phys. Chem. Ref. Data* **2**:757 (1973).
9. J. S. Rowlinson, *Liquids and Liquid Mixtures* (Butterworths, London, 1969), p. 37.
10. W. Wagner, *Eine mathematisch statistische Methode zum Aufstellen thermodynamischer Gleichungen—gezeigt am Beispiel der Dampfdruckgleichung reiner Fluide; Habilitationsschrift TU Braunschweig, FortschrBer VDI-Zeitschriften Reihe 3, Nr. 39* (VDI, Düsseldorf, 1974).
11. N. C. Yang and C. P. Yang, *Phys. Rev. Lett.* **13**:303 (1964).
12. J. W. Magee and J. F. Ely, *Int. J. Thermophys.* **7**:1163 (1986).
13. C. W. Meyer and G. Morrison, *J. Chem. Eng. Data* **36**:409 (1991).
14. C. W. Meyer and G. Morrison, *J. Phys Chem.* **95**:3860 (1991).
15. H. D. Baehr, *Brennstoff-Wärme-Kraft (BWK)* **15**:514 (1963).